Microelectronic Engineering 110 (2013) 250–255

Contents lists available at SciVerse ScienceDirect

Microelectronic Engineering

journal homepage: www.elsevier.com/locate/mee

Enhanced structural and magnetic ordering of FePt/TiO_x bilayers by ion-beam deposition and annealing

Guijun Li [a], Chi Wah Leung [b], Yi-Jing Wu [c], An-Cheng Sun [d], J.-H. Hsu [e], P.T. Lai [a], Ko-Wei Lin [c,*], Philip W.T. Pong [a,*]

[a] Department of Electrical and Electronic Engineering, The University of Hong Kong, Hong Kong
[b] Department of Applied Physics, Hong Kong Polytechnic University, Hong Kong
[c] Department of Materials Science and Engineering, National Chung Hsing University, Taichung, Taiwan
[d] Department of Chemical Engineering & Materials Science, Yuan Ze University, Chung-Li, Taiwan
[e] Department of Physics, National Taiwan University, Taipei, Taiwan

ARTICLE INFO

Article history:
Available online 9 February 2013

Keywords:
FePt
TiO_x
Ion-beam deposition
Annealing
Coercivity

ABSTRACT

The effect of annealing temperature on the microstructure and magnetic properties of FePt/TiO_x bilayers was systemically studied. The grain sizes decreased and the surface roughness increased as the annealing temperatures increased; at the meanwhile, the interface between the FePt and TiO_x layer became more graded, indicating there were more interdiffusion processes as the annealing temperature increased. The coercivity increased as the annealing temperature was raised, indicating more face center tetragonal-phase FePt was formed with higher annealing temperatures. Coercivities over 11 kOe were acquired in both in-plane and out-of-plane directions after annealing at 650 °C for 10 min. TiO_x-capped FePt samples tended to possess higher coercivities after annealing at higher temperatures, which is favorable for high areal density recording applications.

1. Introduction

The superparamagnetic effect of magnetic materials is the main obstacle limiting the increase of magnetic recording density. Typical recording media used these days, such as CoCrPt-based recording media, have poor thermal stability at nanometer scales [1]. Magnetocrystalline anisotropy and grain sizes are the two main factors influencing the thermal stability of a recording medium. Magnetic materials with high magnetocrystalline anisotropy are frequently investigated, such as FePt and CoPt [2–7]. Stoichiometric FePt has two phases at room temperature, fcc phase and fct phase. Fcc phase FePt is superparamagnetic at nanometer scale and it can be synthesized by sputtering. Fct phase FePt is ferromagnetic even in the form of nanoparticles with size down to 4 nm; however, fct–FePt cannot be directly synthesized but must be transformed from fcc phase FePt through annealing [8–16]. The fcc to fct (disorder to order) structural transformation due to annealing is irreversible [17].

The presence of a capping layer can also influence the transformation from fcc to fct-phase of the underlying FePt layer. SiO_2 [18,19], Al_2O_3 [20], Cu [21,22] have been investigated as the capping layer of FePt during annealing. With a single SiO_2 capping layer, 400 °C was sufficient to transform the FePt fcc phase into the fct phase [18]. A 4-nm Cu capping layer, on the other hand, could raise the coercivity of FePt drastically from 3100 Oe to 6000 Oe [22]. Our previous work in FePt/MnO_x has shown that in the reference pure FePt layer, annealing will result in the structure ordering from fcc to fct [23]. TiO_x is also a common capping layer which is very active at diffusion during annealing [24–26]. The interdiffusion between TiO_x and FePt driven by dynamic thermal energy [27] might result in the FePt grains separated by TiO_x boundaries [28]. However, the influence of these high annealing temperatures on the magnetic properties of the TiO_x capped FePt has not been investigated.

In this paper, we investigate the annealing temperature influence on the microstructure and magnetic properties of FePt/TiO_x bilayer. The XRD diffraction patterns, surface morphologies, and magnetic hysteresis measurements of FePt/TiO_x bilayers annealed at different temperatures were studied. Coercivity over 11 kOe has been obtained, which can have important applications in magnetic data recording.

2. Experiment

Silicon substrates were first thermally oxidized to obtain a 180-nm thick SiO_2 layer on top of the silicon substrate, and then

* Corresponding authors. Tel.: +886 4 22851068; fax: +886 4 22857017 (K.W. Lin), tel.: +852 28578491; fax: +852 25598738 (P.W.T. Pong).
E-mail addresses: kwlin@dragon.nchu.edu.tw (K.-W. Lin), ppong@eee.hku.hk (P.W.T. Pong).

0167-9317/$ - see front matter © 2013 Elsevier B.V. All rights reserved.
http://dx.doi.org/10.1016/j.mee.2013.01.042

cleaned with acetone and deionized (DI) water with sonication. Fe and Pt were co-sputtered on the substrate with DC power of 70 W and 33 W, respectively, with the sample stage rotating at 10 rpm/min to form a stoichiometric FePt film with thickness of 10 nm. The base pressure was 8×10^{-9} Torr, and the sputtering Ar pressure was 10 mTorr. A Kaufman source was used to focus the argon ion beam onto a commercial Ti target surface, and an End-Hall source was used to sputter the capping TiO_x layer. The O_2/Ar ratio in the End-Hall ion source was fixed at 30%. No external magnetic field was applied during deposition. The samples were then annealed at 300 °C, 400 °C, 550 °C and 650 °C for 10 min. The crystallinity of the FePt/TiO_x thin films was characterized by grazing angle X-ray diffraction with a Cu K_α source. A JEOL JEM-2010 transmission electron microscopy (TEM) system operating at 200 kV was used for the surface morphology and cross-section characterization. Grain sizes were measured from the TEM images by using an image–analysis software - Image J. Ferromagnetic properties of as-deposited and annealed samples were measured with a LakeShore - 7407 vibrating sample magnetometer (VSM). Surface roughness characterization was carried out using a commercial atomic force microscope (AFM) system.

3. Results and discussion

As-deposited FePt in FePt/TiO_x bilayers exhibited a preferred (1 1 1) orientation with a lattice constant of $a \sim 3.76$ Å as shown in the XRD pattern in Fig. 1. The fct (0 0 1) peak at 25° and the fct (1 1 0) peak at 33°, both being the signature peaks of FePt fct phase [29], are not observed in the as-deposited XRD diffraction in Fig. 1, indicating the absence of the FePt fct phase. As the annealing temperature is increased to 300 °C, the fct (0 0 1) and (1 1 0) peaks were still not observed, while the (1 1 1) peaks were still observed with a lattice constant of $a \sim 3.78$ Å. However, annealing at higher temperatures ranging from 400 °C to 650 °C led to a FePt phase transformation from fcc to fct, as evidenced by the appearance of the (0 0 1) and (1 1 0) fct peaks in the XRD patterns for samples annealed at 400 °C, 550 °C and 650 °C in Fig. 1. Fct (0 0 1) and (2 0 0) peaks were observed at 400 °C, and enhanced intensities of these two peaks were found at 550 °C and 650 °C, indicting the fct phase transformation is enhanced as the annealing temperature increased. The amount of fct phase can be implied using the order parameters [30] of fct phase FePt, which was calculated by

$$S = \sqrt{\frac{\left[I_{(1\,1\,0)}/I_{(1\,1\,1)}\right]_{measured}}{\left[I_{(1\,1\,0)}/I_{(1\,1\,1)}\right]_{S=1}}}$$

where the $I_{(1\,1\,0)}$ and $I_{(1\,1\,1)}$ stands for the intensity of the XRD peak of fct phase (1 1 0) and (1 1 1) peaks, the numerators are experimentally measured from the sample and the denominators are the calculated results from an ideal sample with order parameter S of 1. The order parameter was 0.74 for FePt/TiO_x bilayer annealed at 550 °C and 0.78 for sample after annealing at 650 °C, calculated from the intensities of the fct (1 1 1) and (1 1 0) peaks in Fig. 1. The characteristic peak of fct phases (such as (0 0 1) and (0 0 2)) started to come out after annealing at 400 °C, and get stronger through annealing at 550 °C and 650 °C; at the meanwhile, the characteristic peak of fcc phase started to disappear after annealing at 400 °C and there is little fcc phase peak after annealing at temperature on either 550 °C or 650 °C. This indicates that the ordered FePt structures could be achieved by co-sputtering Fe and Pt and the post-annealing above 400 °C in the FePt/TiO_x bilayer structure. Annealing with higher temperatures lead to more fct phase transformed from fcc phase.

The effect of the TiO_x capping layer on microstructure and magnetic properties of FePt was studied by analyzing the interfaces. To understand the microstructure and surface morphology of the samples, high-resolution TEM (HRTEM) was used to characterize the FePt/TiO_x bilayers. Bright field images and the electron diffraction patterns of FePt/TiO_x bilayers, after annealing at different temperatures, are displayed in Fig. 2. The electron diffraction patterns are found to be the mixed structures of fcc and fct FePt phases; however, the appearance of the fct phase feature peaks such as fct phase (0 0 1) and (0 0 2) indicate the phase transformation from fcc to fct FePt even though the films may still be mixture of fcc and fct phases. As-deposited FePt/TiO_x bilayers exhibit a polycrystalline structure with grain sizes ranging from 5 to 12 nm, as measured from Fig. 2(a). Polycrystalline structure can be observed in the as-deposited FePt/TiO_x, as indicated in the electron diffraction pattern in the inset of Fig. 2(a). The grain size grew significantly to the range of 16–40 nm after annealing at 400 °C for 10 min (Fig. 2(b)). Ordered fct FePt phases as indexed by electron diffraction patterns are observed in the inset of Fig. 2(b), indicating that there is more fct phase formation than the as-deposited sample, where no obvious fct phase was observed. Similar surface morphology is also observed in FePt/TiO_x bilayers after annealing at 550 °C, with a wider

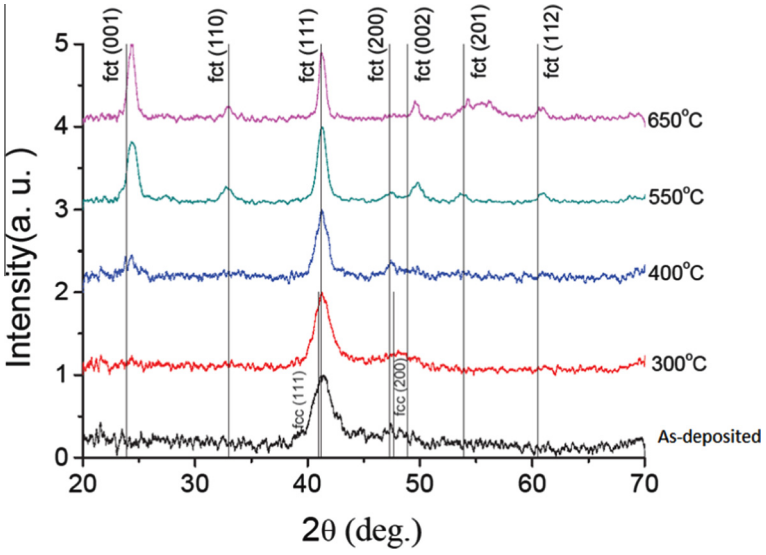

Fig. 1. XRD diffraction patterns of FePt/TiO_x bilayer with different annealing temperatures. Labels are identified by the JCPDS card.

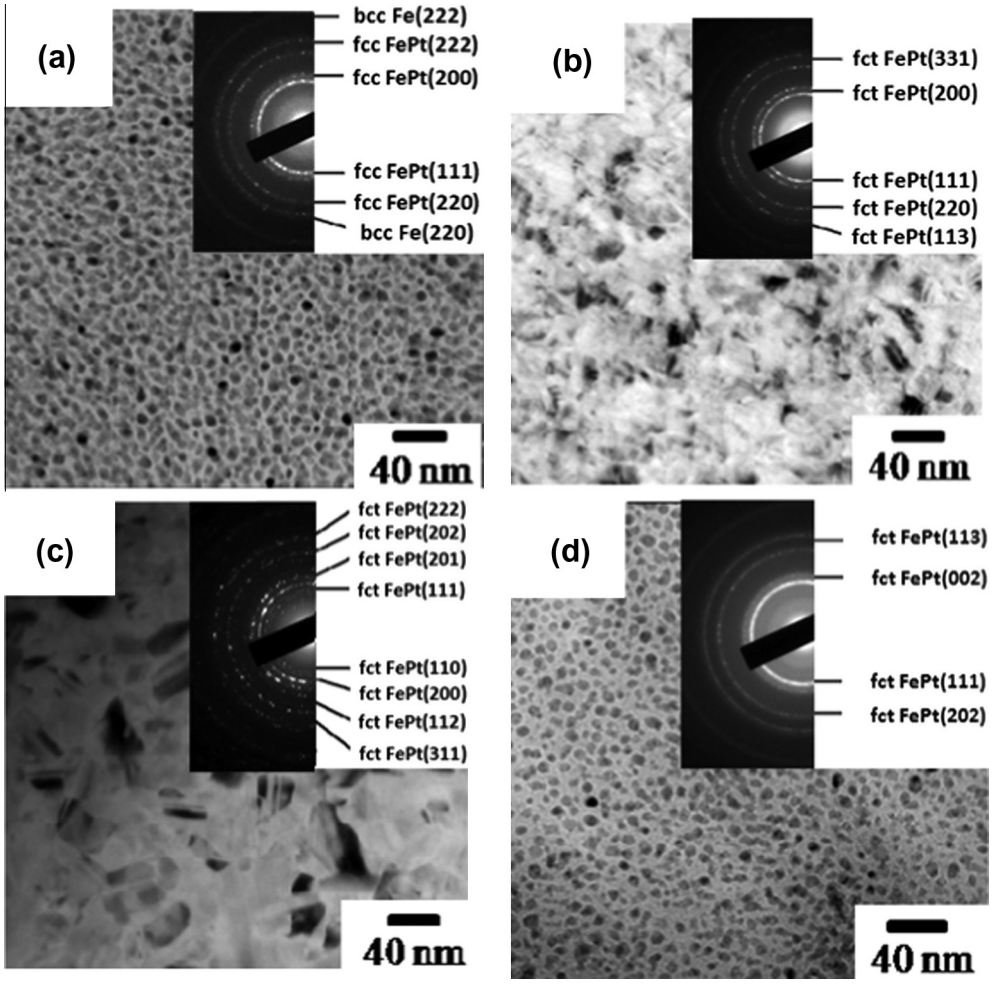

Fig. 2. Bright field images and electron diffraction patterns of FePt/TiO_x bilayer with different annealing temperatures. (a) As-deposited (b) 400 °C (c) 550 °C (d) 650 °C.

grain size distribution ranging from 6 nm to 50 nm (Fig. 2(c)). Fct phases such as (201) and (112) orientations are observed in the electron diffraction patterns in the inset of Fig. 2(c), indicating more fct phase formation after annealing at 550 °C for 10 min compared with previous samples annealed with lower temperatures. In contrast, after annealing at 650 °C for 10 min, separated grains appear with similar sizes as shown in Fig. 2(d). Electron diffraction patterns in the inset of Fig. 2(d) exhibit (002), (202), and (113) orientations of fct phase shown in the inset of Fig. 2(d), indicating there is much more fct phase formed than the previous ones. The grain size distribution after annealing at 650 °C is plotted in Fig. 3 and the grain sizes mostly concentrate in the range from 5 nm to 8 nm. This grain size distribution is narrower than the distributions in the other samples annealed at lower temperatures.

In order to investigate the influence of TiO_x diffusion into FePt on the microstructure of bilayers, TEM cross-section characterization was performed and the results are shown in Fig. 4. As-deposited FePt/TiO_x bilayer exhibits a clear interface separating the 10 nm FePt and 9 nm TiO_x films (Fig. 4(a)). When the annealing temperature is increased, the interface between FePt and TiO_x layer becomes less clear. The TEM cross-section image of interface of FePt/TiO_x bilayer after annealing at 400 °C is shown in Fig. 4(b) and the interface between FePt and TiO_x becomes graded. After annealing at 550 °C, the interface in Fig. 4(c) becomes less evident and FePt and TiO_x layers almost mix together. This result indicates that as the annealing temperature is increased, there is enhanced

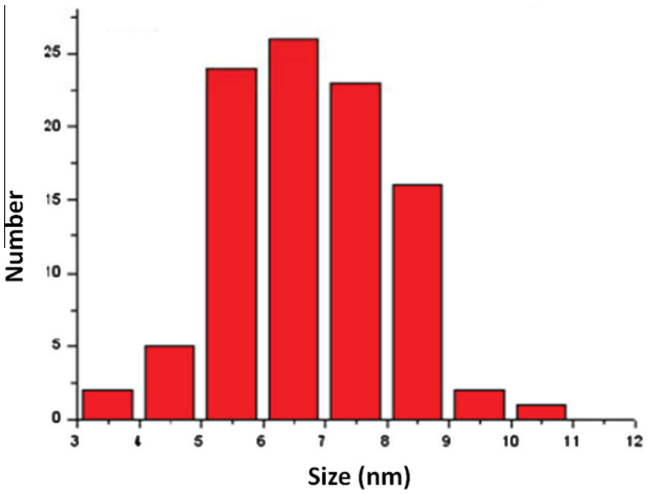

Fig. 3. Grain size distribution of FePt/TiO_x after annealing at 650 °C for 10 min.

diffusion at the FePt and TiO_x interface. FePt/TiO_x bilayer after annealing at 650 °C for 10 min exhibited the most graded interface (Fig. 4(d)), indicating there was strong diffusion at the FePt and TiO_x interface and there was even diffusion between FePt and substrate

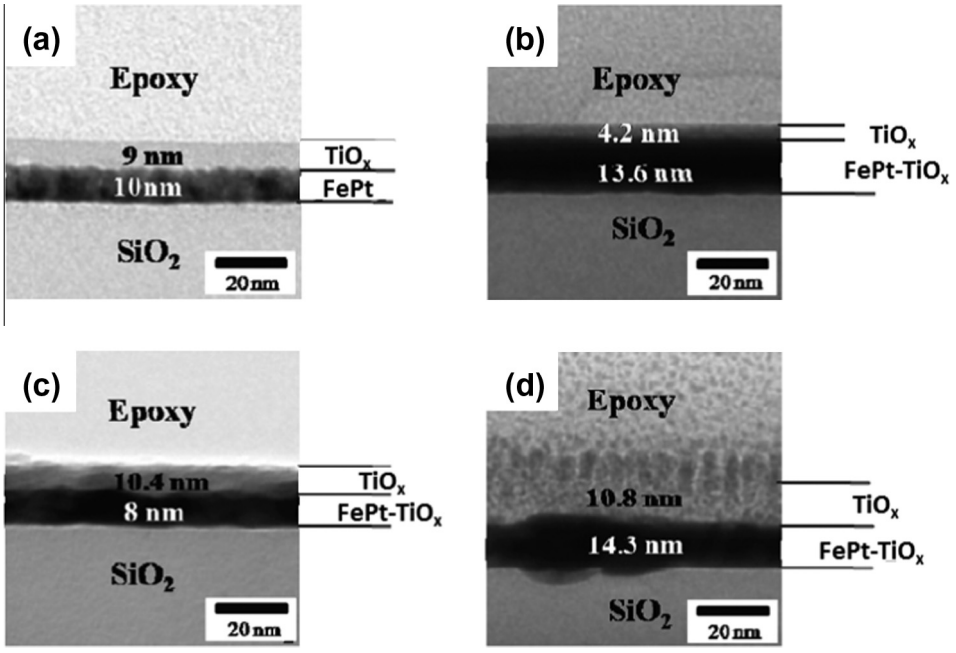

Fig. 4. TEM cross-section image of FePt/TiO_x bilayer. (a) As-deposited (b) After annealing at 400 °C (c) After annealing at 550 °C (d) After annealing at 650 °C.

SiO_2. Thus the small grain sizes are mainly contributed by the diffusion in Figs. 2(d) and 3 after annealing at 650 °C for 10 min.

To further investigate the extent of diffusion between FePt and TiO_x layers, X-ray photoelectron spectroscopy (XPS) was performed and the depth profile is shown in Fig. 5 as a function of sputter time where the layer boundaries were decided by the atomic concentration. In the figure, the *x*-axis corresponds to the sputtering time and the *y*-axis is the atomic concentration of each element obtained using atomic sensitive factor. The XPS results have shown the similar 50–50 atomic composition in Fe and Pt qualitatively

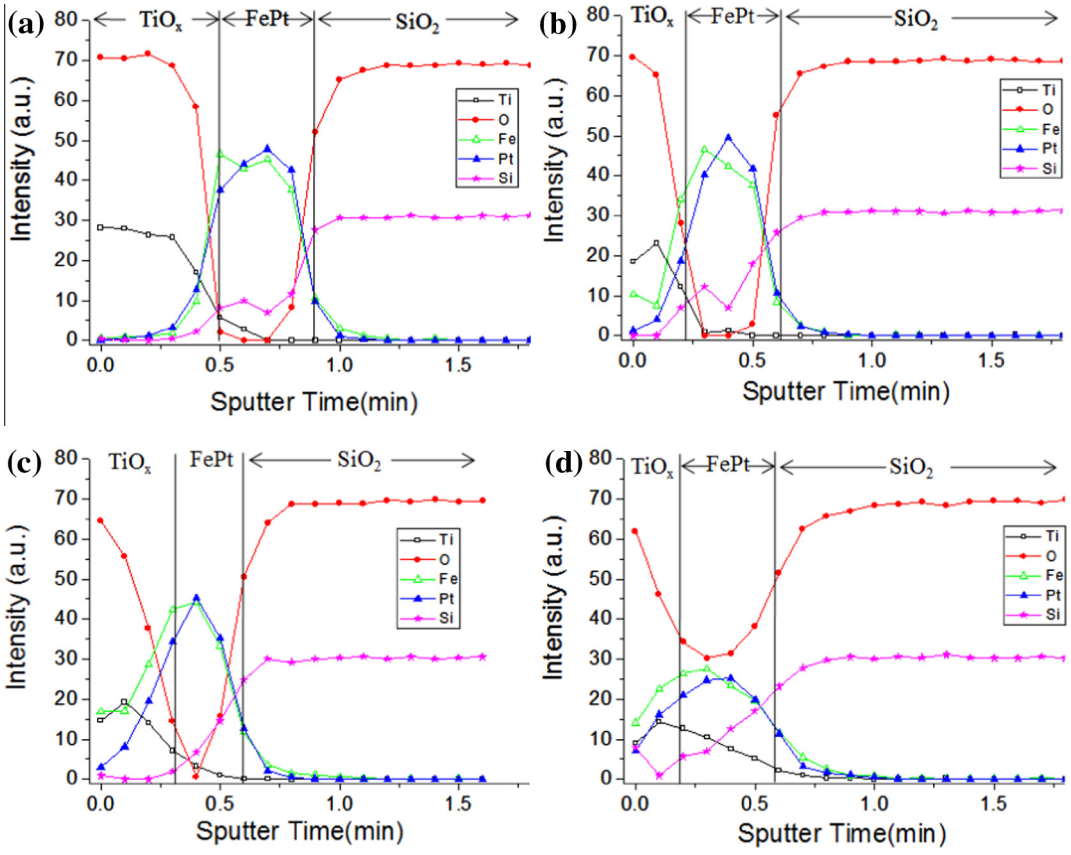

Fig. 5. XPS depth profile of FePt/TiO_x bilayer after annealing at different temperatures. (a) As-deposited (b) 400 °C (c) 550 °C (d) 650 °C.

Table 1
Surface roughness of FePt/TiO_x with different annealing temperatures with scanning area of 2 × 2 μm.

T (°C)	25	300	400	550	650
Roughness (nm) (scanning area: 2 × 2 μm)	0.38	0.34	0.51	0.51	1.21

as in [31]. As-deposited FePt/TiO_x bilayer (Fig. 5(a)) shows a sharp transition at 0.5 min, around which Ti and O concentrations drop strongly and the Fe and Pt contents show marked increases. As the annealing temperature is increased to 400 °C, the transition becomes less distinct and moved left to 0.3 min in Fig. 5(b). There is Fe and Pt observed to the left of the interface, indicating that some FePt already diffused into TiO_x after annealing at 400 °C. As the annealing temperature further increased to 550 °C more Fe and Pt can be observed over a wider range of sputtering time (from 0 min to 0.3 min), indicating more FePt diffused into TiO_x after annealing at 550 °C compared with the previous samples annealed at lower temperatures. For the sample annealed at 650 °C (Fig. 5(d)), the interface widened even more and moved further left to 0.2 min. Different from the previous XPS data for samples with lower annealing temperatures (where a sharp interface could be observed), the Ti, O, Fe and Pt are observed over the whole bilayer sample, indicating that there is strong diffusion both from FePt into TiO_x and vice versa.

The surface morphology of FePt/TiO_x bilayer was also investigated with atomic force microscopy with a scanning area of 2 × 2 μm. The roughness of sample surface with different annealing temperatures is given in Table 1. As the annealing temperature is increased from room temperature to 650 °C, the surface roughness first slightly decreases to 0.34 nm at 300 °C, and then increases up to 1.21 nm at 650 °C. This result indicates that annealing temperature higher than 300 °C leads to the formation and grain growth of fct phase FePt, implying a surface roughness increase.

To correlate the microstructure and the magnetism of the FePt/TiO_x bilayer, hysteresis loops were measured with VSM at room temperature. The coercivities in both in-plane and out-of-plane directions of the FePt/TiO_x bilayers, after annealing at different temperatures, are summarized in Fig. 6. The as-deposited bilayer sample exhibits relatively small coercivity of 100 Oe, both in the in-plane and out-of plane directions. After annealing at 300 °C, FePt is still present in the fcc phase (Fig. 1), and is reflected from the relatively small coercivities (800 Oe in the out-of-plane direction, 300 Oe in the in-plane direction). Further increasing the annealing temperature to 400 °C leads to the formation of fct–FePt, which is evidenced from the relatively large coercivity of 3 kOe (3.5 kOe) in the in-plane (out-of-plane) direction. Further increasing the annealing temperature lead to even more fct phase, characterized by the coercivity of 9.5 kOe in the out-of-plane direction and 10 kOe in the in-plane direction. After annealing at 650 °C, coercivity of 11.4 ± 0.2 kOe in the out-of-plane direction and 11.7 ± 0.2 kOe in the in-plane direction indicated that there was even more fct phase formed. These results show that the coercivity tended to increase with the annealing temperature, indicating there was more fct phase formed due to annealing. This coincided with results obtained by the XRD and TEM in Figs. 1 and 2 where they all show more fct phase formed as the annealing temperature increased, confirming that the fct to fcc ratio increased as the annealing temperature increased from room temperature to 650 °C.

From the microstructure and magnetic properties of FePt/TiO_x bilayers annealed at different temperatures, it is concluded that the TiO_x capping layer after annealing would form oxide boundaries and separate the FePt grains. Highest coercivity of 11.4 ± 0.2 kOe in the out-of-plane direction and 11.7 ± 0.2 kOe in the in-plane direction after annealing at 650 °C for 10 min were achieved.

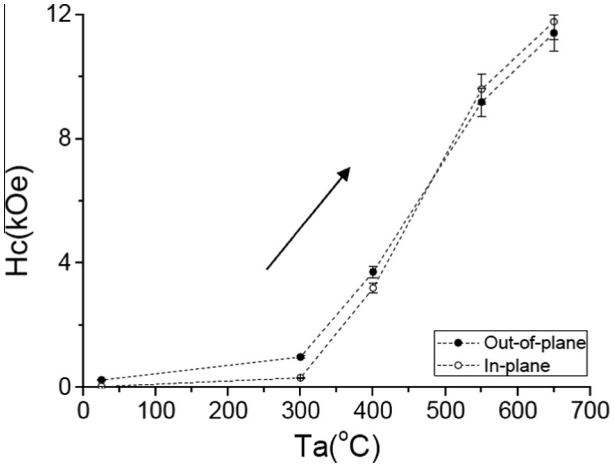

Fig. 6. Coercivity and annealing temperature relationship of FePt/TiO_x bilayer after annealing at different temperatures.

The above results show that through annealing, the ordering of FePt can be achieved from fcc to fct phase. Meanwhile, the interdiffusion can effectively separate the FePt grains with TiO_x. Compared to other oxides, such as SiO_2 [32] and MnO_x [23], the TiO_x have different impacts on the magnetic properties due to different reactivity and interdiffusion with FePt layers. The active diffusion of TiO_x can effectively constitute TiO_x boundaries and separate the FePt grains to form granular-structured FePt films [23,32], which may have important applications in future high-density magnetic recording media.

4. Conclusion

The influence of annealing temperature on the microstructure and magnetic properties of FePt/TiO_x bilayers was investigated. The magnetic properties and microstructure of FePt capped with TiO_x layer could be modified with annealing temperature. The different annealing temperature influences the FePt structure by transforming it from fcc to fct phase and also by diffusing TiO_x into FePt as oxides boundaries during annealing. Highest coercivities with 11.4 ± 0.2 kOe in the out-of-plane direction and 11.7 ± 0.2 kOe in the in-plane direction after annealing at 650 °C for 10 min were achieved. Annealing at 650 °C was sufficient to transform FePt fcc into fct phase and also caused TiO_x diffusing into FePt, separating the continuous FePt thin films into individual grains.

Acknowledgements

This work was supported in part by the Seed Funding Program for Basic Research from the University of Hong Kong, the RGC-GRF grant (HKU 7049/11P), the RGC-GRF grant (PolyU 5232/09E) and PolyU Grant A-PL51, the University Grants Council of Hong Kong (Contract No. AoE/P-04/08), and ITF Tier 3 funding (ITS/112/12) and the Ministry of Economic Affairs of Taiwan and National Science Council of Taiwan.

References

[1] K. Srinivasan, S.N. Piramanayagam, R. Sbiaa, R.W. Chantrell, J. Magn. Magn. Mater. 320 (2008) 3041–3045.
[2] K. Barmak, J. Kim, S. Shell, E.B. Svedberg, J.K. Howard, Appl. Phys. Lett. 80 (2002) 4268–4270.
[3] M.R. Visokay, R. Sinclair, Appl. Phys. Lett. 66 (1995) 1692–1694.

[4] H. Zeng, M.L. Yan, N. Powers, D.J. Sellmyer, Appl. Phys. Lett. 80 (2002) 2350–2352.
[5] S. Jeong, Y.N. Hsu, D.E. Laughlin, M.E. McHenry, IEEE Trans. Magn. 36 (2000) 2336–2338.
[6] S. Jeong, Y.N. Hsu, D.E. Laughlin, M.E. McHenry, IEEE Trans. Magn. 37 (2001) 1299–1301.
[7] J.M. MacLaren, R.R. Duplessis, R.A. Stern, S. Willoughby, IEEE Trans. Magn. 41 (2005) 4374–4379.
[8] H.Y. Wang, X.K. Ma, Y.J. He, S. Mitani, M. Motokawa, Appl. Phys. Lett. 85 (2004) 2304–2306.
[9] K. Aimuta, K. Nishimura, S. Hashi, M. Inoue, IEEE Trans. Magn. 41 (2005) 3898–3900.
[10] T. Seki, T. Shima, K. Yakushiji, K. Takanashi, G.Q. Li, S. Ishio, IEEE Trans. Magn. 41 (2005) 3604–3606.
[11] A. Yano, T. Koda, S. Matsunuma, IEEE Trans. Magn. 41 (2005) 3211–3213.
[12] F. Albertini, L. Nasi, F. Casoli, S. Fabbrici, P. Luches, A. Rota, S. Valeri, J. Magn. Magn. Mater. 316 (2007) E158–E161.
[13] Y. Inaba, K.L. Torres, A. Cole, R. Vanfleet, R. Ott, T. Klemmer, J.W. Harrell, G.B. Thompson, J. Magn. Magn. Mater. 321 (2009) 2451–2458.
[14] H. Ito, T. Kusunoki, H. Saito, S. Ishio, J. Magn. Magn. Mater. 272–276 (2004) 2180–2181.
[15] N. Murayama, S. Soeya, Y. Takahashi, M. Futamoto, J. Magn. Magn. Mater. 320 (2008) 3057–3059.
[16] H. Zeng, S.H. Sun, R.L. Sandstrom, C.B. Murray, J. Magn. Magn. Mater. 266 (2003) 227–232.
[17] M.V. Mansilla, J. Gomez, E.S. Leva, F.C. Gamarra, A.A. Barahona, A. Butera, J. Magn. Magn. Mater. 321 (2009) 2941–2945.
[18] D.H. Wei, Y.D. Yao, IEEE Trans. Magn. 45 (2009) 4092–4095.
[19] Y. Ding, D.H. Wei, Y.D. Yao, J. Appl. Phys. 103 (2008) 07E145.
[20] Y.K. Takahashi, K. Hono, Appl. Phys. Lett. 84 (2004) 383–385.
[21] D.H. Wei, Y.D. Yao, Inec: 2010 3rd International Nanoelectronics Conference, Vols 1 and 2, (2010) 704–705.
[22] J.S. Chen, J.P. Wang, J. Magn. Magn. Mater. 284 (2004) 423–429.
[23] A.C. Sun, H.F. Hsu, H.J. Wu, J.H. Hsu, P.W.T. Pong, T. Suzuki, K.W. Lin, IEEE T. Magn. 47 (2011) 501–504.
[24] A. Francois, V. Aimez, J. Beauvais, M. Gendry, P. Regreny, Appl. Phys. Lett. 89 (2006) 164107.
[25] C.J. Liu, J.S. Chen, Appl. Phys. Lett. 80 (2002) 2678–2680.
[26] D.J. Kirk, D.J.H. Cockayne, A.K. Petford-Long, G. Yi, J. Appl. Phys. 106 (2009) 123915.
[27] A.C. Sun, H.F. Hsu, Y.J. Wu, Y.L. Chiu, J.H. Hsu, P.W.T. Pong, T. Suzuki, K.W. Lin, Jpn. J. Appl. Phys. 49 (2010) 123001.
[28] C.J. Jiang, J.S. Chen, J.F. Hu, G.M. Chow, J. Appl. Phys. 107 (2010) 123915.
[29] M. Mito, Y. Komorida, N.J.O. Silva, H. Tsuruda, H. Deguchi, S. Takagi, T. Tajiri, T. Iwamoto, Y. Kitamoto, J. Appl. Phys. 108 (2010) 124315.
[30] T. Shima, T. Moriguchi, S. Mitani, K. Takanashi, Appl. Phys. Lett. 80 (2002) 288–290.
[31] C.M. Kuo, P.C. Kuo, H.C. Wu, J. Appl. Phys. 85 (1999) 2264–2269.
[32] K.W. Lin, Y.L. Chiu, A.C. Sun, J.H. Hsu, J. van Lierop, T. Suzuki, Jpn. J. Appl. Phys. 48 (2009) 073002.